

# Application of underdamped Langevin dynamics simulations for the study of diffusion from a drug-eluting stent

Shaked Regev<sup>1</sup> and Oded Farago<sup>1,2</sup>

<sup>1</sup>*Department of Biomedical Engineering, Ben-Gurion University of the Negev, Be'er Sheva 85105, Israel*

<sup>2</sup>*Ilse Katz Institute for Nanoscale Science and Technology,  
Ben-Gurion University of the Negev, Be'er Sheva 85105, Israel*

We use a one-dimensional two layer model with a semi-permeable membrane to study the diffusion of a therapeutic drug delivered from a drug-eluting stent (DES). The rate of drug transfer from the stent coating to the arterial wall is calculated by using underdamped Langevin dynamics simulations. Our results reveal that the membrane has virtually no delay effect on the rate of delivery from the DES. The work demonstrates the great potential of underdamped Langevin dynamics simulations as an easy to implement, efficient, method for solving complicated diffusion problems in systems with a spatially-dependent diffusion coefficient.

## I. INTRODUCTION

Arterial stents are indispensable in the treatment of coronary artery disease (CAD) and more specifically stenosis, the abnormal narrowing of blood vessels [1]. These stents are frequently implanted in arteries where blood flow has become precariously impeded. In recent decades, they have revolutionized the treatment of stenosis by providing a safer alternative to coronary surgery. In addition to diminishing the risk of major surgery complications, stents also facilitate recovery and avoid administering general anesthesia to patients [2]. However, arterial stents have only been able to reduce the instances of recurring stenosis, or restenosis, to 20-30%, compared to 30-40% in coronary surgery [3].

In an effort to further curtail these rates, drug-eluting stents (DES) were introduced. A DES is a stent that uses programmed pharmacokinetics to release anti-proliferative pharmaceuticals into the arterial wall. It is comprised of a metallic strut coated with a polymeric matrix or gel that encapsulates the therapeutic drug [4]. The drug reduces smooth muscle cell growth and prevents an inflammatory response - two predominant causes of in-stent-restenosis and neo-intima proliferation [4]. Stents coated in anti-proliferative agents have mitigated instances of restenosis to roughly 5% in clinical trials and are FDA approved [5].

Understanding the rate at which drugs are transported through the arterial tissue is crucial for stent design, and as such has been studied extensively [6–33]. It has been identified that the major mechanism of drug transfer from the coating is diffusion through the arterial wall [34]. Thus, advective forces arising, e.g., from blood circulation in the arteries have been ignored in many models. The simplest model describing the system is based on the solution of a diffusion equation in a two-layer one-dimensional system. One-dimensional models represent a mathematical idealization of the three-dimensional stent geometry; nevertheless, they dominate the theoretical literature on the subject because the drug release is predominantly along the normal direction to the stent axis whose dimension (the stent thickness) is much smaller

than the lateral dimension (the stent radius). More complex one-dimensional models give weight to other phenomena and factors such as chemical reactions between the drug and the arterial wall [7–15], directed advection of the drug [7–9, 12–21], cell metabolism [16, 19], and the drug topcoat membrane permeability [6, 12, 14, 22, 23]. These phenomena and factors amend the partial differential equations (PDEs) that describe the transport of the drug. They also modify the boundary conditions between the layers and often require the introduction of additional layers [7, 8, 17, 20, 22, 24–27]. Some studies consider more complex two- [15, 26, 28] and even three-dimensional [13, 19, 22, 29, 30] geometries. The PDEs are often solved by separation of variables, or numerically through some kind of a discretization scheme, e.g., finite elements, finite differences, and the marker cell method. Noteworthy exceptions include analytical Laplace transform solutions [27], Boltzmann reductions [11], and numerically solved Volterra integral equations [23]. Experimental data is also available [31–33], and has been used to test and validate theoretical models.

Layered systems, where in each region the diffusion coefficient takes a different value, constitute a subclass of a more general class of systems with spatially varying diffusivity:  $D = D(x)$ . Diffusion in such systems is described by Fick's second law

$$\frac{\partial P(x, t)}{\partial t} = -\frac{\partial J(x, t)}{\partial x} = \frac{\partial}{\partial x} \left( D(x) \frac{\partial P(x, t)}{\partial x} \right), \quad (1)$$

where  $P(x, t)$  is the probability of being at coordinate  $x$  at time  $t$ , and  $J(x, t) = -D(x)\partial_x P(x, t)$  is the probability flux. An alternative route for calculating  $P(x, t)$  is to numerically integrate the corresponding Langevin equation [36]

$$m \frac{dv}{dt} = -\alpha(x)v + \beta(x(t)), \quad (2)$$

where  $m$  and  $v$  denote, respectively, the mass and velocity of a diffusing particle. Langevin's equation describes Newtonian dynamics under the action of two effective forces: friction [first term on the r.h.s. of Eq. (2)]

and stochastic thermal noise (second term). The friction coefficient  $\alpha(x)$  in (2) is related to the diffusivity  $D(x)$  in (1) via Einstein's relation  $\alpha(x) = k_B T / D(x)$  [37, 38], where  $T$  is the temperature of the system and  $k_B$  is Boltzmann's constant. The stochastic noise,  $\beta$ , is chosen from a Gaussian distribution with zero mean  $\langle \beta(x(t)) \rangle = 0$ , and delta-function auto-correlation  $\langle \beta(t)\beta(t') \rangle = 2k_B T \alpha(x(t))\delta(t-t')$  [38, 39]. The probability density function (PDF) of the particle,  $P(x, t)$ , can be computed from an ensemble of simulated trajectories, where the initial position of the particle at each trajectory is chosen from the initial PDF  $P(x, 0)$ .

The accuracy of the Langevin dynamics simulation method for computing  $P(x, t)$  depends largely on the quality of the discrete-time numerical integrator. Here (as in previous works [40]), we use the efficient and robust method of Grønbech-Jensen and Farago (G-JF) [35, 41] in combination with the ‘‘inertial’’ convention [38, 39] for choosing the value of  $\alpha$ . In the absence of conservative forces from a potential energy gradient (which is the case discussed throughout this paper), the G-JF integrator employs the following set of equations

$$x^{n+1} = x^n + bdtv^n + \frac{bdt}{2m}\beta^{n+1}, \quad (3)$$

$$v^{n+1} = av^n + \frac{b}{m}\beta^{n+1}, \quad (4)$$

to advance the coordinate  $x^n = x(t_n)$  and velocity  $v^n = v(t_n)$  by one time step from time  $t_n = ndt$  to  $t_{n+1} = t_n + dt$ . In the above G-JF equations (3)-(4),  $\beta^{n+1}$  is a Gaussian random number satisfying

$$\langle \beta^n \rangle = 0; \quad \langle \beta^n \beta^l \rangle = 2\alpha k_B T dt \delta_{n,l}, \quad (5)$$

and the damping coefficients of the algorithm are

$$b = [1 + (\alpha dt / 2m)]^{-1}; \quad a = [1 - (\alpha dt / 2m)]b. \quad (6)$$

Since the friction varies in space, the integrator must be complemented with a convention for choosing the value of  $\alpha$  to be used in Eqs.(5) and (6) at each time step. The ambiguity concerning the appropriate choice of  $\alpha$  is known in the literature as the ‘‘Itô-Stratonovich dilemma’’ [42–44]. Here, we use the recently proposed inertial convention [38, 39] that assigns to  $\alpha$  the value of the spatial average of  $\alpha(x)$  along the inertial trajectory from  $x^n$  to  $\tilde{x}^{n+1} = x^n + v^n dt$

$$\bar{\alpha} \equiv \frac{\int_{x^n}^{\tilde{x}^{n+1}} \alpha(x) dx}{\tilde{x}^{n+1} - x^n} = \frac{A(\tilde{x}^{n+1}) - A(x^n)}{\tilde{x}^{n+1} - x^n}, \quad (7)$$

where  $A(x)$  is the primitive function of  $\alpha(x)$ . We have previously demonstrated that while any reasonable convention for choosing  $\alpha$  yields the correct PDF at the limit of infinitesimally small time step  $dt \rightarrow 0$ , the inertial convention gives very accurate results even for relatively large time steps. This property of the inertial convention stems from the fact that at small time scales,  $dt \ll m/\alpha$ , the inertial trajectory serves as the leading approximation to the actual path of the particle.

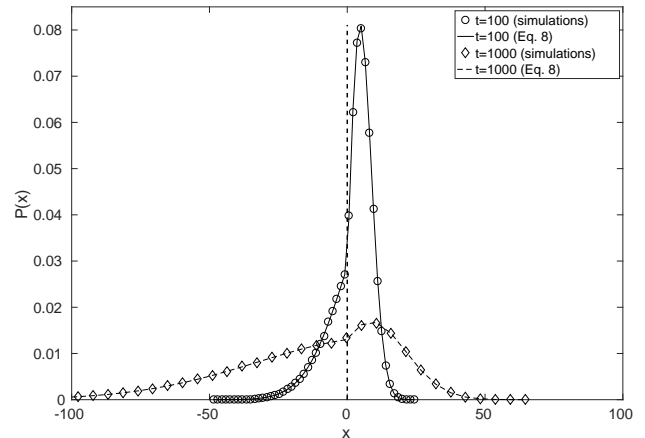


FIG. 1: The PDF of the two-layer problem (the vertical line at  $x = 0$  represents the interface). Open circles and the solid line denote, respectively, the results of the Langevin dynamics simulations and the analytical solution Eq. (8) at  $t = 100$ . Similarly, the open diamonds and the dashed line denote results for  $t = 1000$ .

## II. TWO-LAYER SYSTEMS

Assuming in Eq. (1) that  $0 < D(x) < \infty$  ( $-\infty < x < \infty$ ), the resulting  $P(x, t)$  (for  $t > 0$ ) must be a continuous function for any initial condition. The flux  $j(x, t) = -D(x)\partial_x P(x, t)$  must also be continuous if no source or sink of probability are present in the system. These properties of the PDF also apply to layered systems where  $D$  is piece-wise constant. In this paper, we consider a simple one-dimensional two-layer model for a DES. Before arriving at that model, we first consider the simplest two-layer system, where  $D(x) = D_1$  for  $x < 0$  and  $D(x) = D_2$  for  $x > 0$ . As just stated above, both the PDF and the flux must be continuous, including at  $x = 0$ , which sets the boundary conditions at the interface between the layers. Assuming that a particle is initially located at  $x = x_0 > 0$ , i.e.,  $P(x, 0) = \delta(x - x_0)$ , then the *normalized* (i.e., satisfying  $\int_{-\infty}^{\infty} P(x, t) dx = 1$ ) solution of (1) for  $t > 0$  is given by

$$P(x, t) = \begin{cases} \frac{A}{\sqrt{4\pi D_1 t}} e^{-\frac{(x-x_1)^2}{4D_1 t}} & x < 0 \\ \frac{1}{\sqrt{4\pi D_2 t}} e^{-\frac{(x-x_0)^2}{4D_2 t}} + \frac{B}{\sqrt{4\pi D_2 t}} e^{-\frac{(x+x_0)^2}{4D_2 t}} & x > 0, \end{cases} \quad (8)$$

with  $x_1 = x_0 \sqrt{D_1/D_2}$ ,  $A = 2/(1 + \sqrt{D_2/D_1})$ , and  $B = (1 - \sqrt{D_1/D_2})/(1 + \sqrt{D_1/D_2})$ . This solution can be interpreted as follows: For  $x > 0$ , the PDF is the outcome of two diffusion processes associated with (i) the original particle which has a unity weight and is located at  $x = x_0$ , and an image particle of weight  $B$  located at  $x = -x_0$ . For  $x < 0$ , the PDF represents diffusion of an image particle of weight  $A = 1 - B$ , which is located at  $x = x_1$ . Notice that for  $D_1 = D_2$ , we have  $x_1 = x_0$ ,  $A = 1, B = 0$ , which reduces Eq. (8) to the well-

known Gaussian solution for a particle diffusing in an infinite space with constant diffusivity. Fig. 1 compares the PDF (8) for  $D_1 = 1$ ,  $D_2 = 0.1$ , and  $x_0 = 4$  (lines) to the results of Langevin dynamics simulations based on the above described G-JF integrator with the inertial convention (symbols). In the simulations, we set  $m = 1$  and  $k_B T = 1$ . Thus, the friction coefficients in the layers are given by  $\alpha_1 = k_B T / D_1 = 1$  and  $\alpha_2 = k_B T / D_2 = 10$ . We set the time step to  $dt = 0.1$ . For both layers, this value of  $dt$  satisfies the condition  $dt \leq 2m/\alpha$ , which has been assumed in the application of the inertial convention for choosing  $\bar{\alpha}$  (see discussion at the end of section I). Fig. 1 depicts the PDF at  $t = 100$  and  $t = 1000$ , based on  $2.5 \times 10^5$  trajectories. The total CPU time of the simulations was 3 minutes on a PC. The agreement with Eq. (8) is excellent. Interestingly, we obtained almost identical results with  $dt = 4$ , which does not satisfy the condition for inertial dynamics. In the latter case, the total duration of the simulations was 5 seconds.

Two interesting limiting cases may be considered: For  $D_2/D_1 \rightarrow \infty$  ( $D_2 = D$ ,  $D_1 \rightarrow 0$ ), we have  $B \rightarrow 1$ , and

$$P(x, t) = \frac{1}{\sqrt{4\pi D_2 t}} e^{-\frac{(x-x_0)^2}{4D_2 t}} + \frac{1}{\sqrt{4\pi D_2 t}} e^{-\frac{(x+x_0)^2}{4D_2 t}} \quad (x > 0), \quad (9)$$

which is the solution of the same problem with a reflecting wall at the origin. To simulate Langevin dynamics in the presence of a reflecting wall (located, without loss of generality, at  $x = 0$ ), we follow the trajectory of the particle as computed by the Langevin integrator. If it crosses the wall, i.e., when  $x^{n+1} < 0$ , we simply relocate the particle at  $-x^{n+1} > 0$ , and reverse the velocity from  $v^{n+1}$  to  $-v^{n+1}$ . The other limiting case is  $D_2/D_1 \rightarrow 0$  ( $D_2 = D$ ,  $D_1 \rightarrow \infty$ ). Here, we have  $B \rightarrow -1$ , and

$$P(x, t) = \frac{1}{\sqrt{4\pi D_2 t}} e^{-\frac{(x-x_0)^2}{4D_2 t}} - \frac{1}{\sqrt{4\pi D_2 t}} e^{-\frac{(x+x_0)^2}{4D_2 t}} \quad (x > 0), \quad (10)$$

which is the solution of the same problem with an absorbing wall at the origin. When one simulates Langevin dynamics with absorbing boundaries, the trajectory is terminated when it crosses the boundary. Obviously, the total probability is not conserved but rather diminishes with time.

### III. SEMI-PERMEABLE MEMBRANE

Drug-eluting stents include a topcoat that influences the rate of drug release to the artery. Since the topcoat layer is thin compared to the dimensions of the stent and the arterial wall, it can be included in a DES two-layer model as a semi-permeable membrane boundary that controls the transition rate from the coating (first layer) to the artery (second layer). Let us first discuss the problem of diffusion across a semi-permeable membrane within the general context of two-layer systems. We denote by  $P_{\text{cross}}$  the probability that, within a small time interval  $dt$ , a drug molecule arriving to the boundary from the first layer crosses it to the second layer.

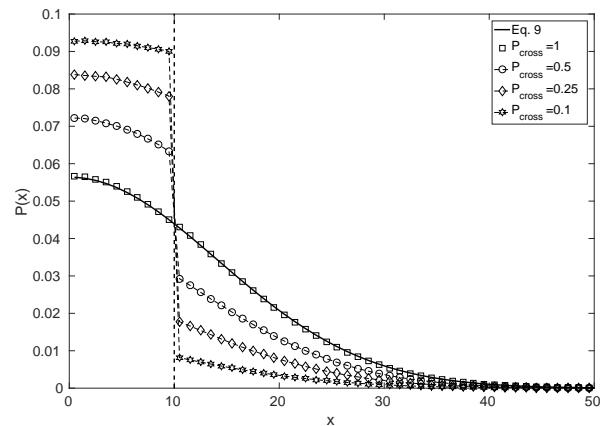


FIG. 2: The PDF at  $t = 100$  of a particle starting next to a reflecting wall at the origin, and diffusing through a semi-permeable membrane at  $x = 10$  (represented by the vertical line), with crossing probability  $P_{\text{cross}}$ . Squares, circles, diamonds and stars denote the results of the Langevin dynamics simulations for  $P_{\text{cross}} = 1, 0.5, 0.25, 0.1$ , respectively. The solid line shows the solution for the case with no membrane [see Eq. (9)].

In the opposite direction (from the second layer back to the first), the crossing probability is unity. A semi-permeable membrane can be incorporated in Langevin dynamics simulations of layered systems in the following manner: Let us first consider the simpler case where the friction coefficient  $\alpha$  is the same on both sides of the membrane, which is located at  $x = x_m$ . We follow the particle until it crosses the membrane ( $x^n < x_m$  and  $x^{n+1} > x_m$ ). In order to decide whether the particle should cross the boundary or be reflected from it, we draw a random number,  $R$ , from a uniform distribution between zero and one. We accept the new coordinate and velocity  $(x^{n+1}, v^{n+1})$  if  $R < P_{\text{cross}}$  (crossing), and reverse them to  $(2x_m - x^{n+1}, -v^{n+1})$  if  $R > P_{\text{cross}}$  (reflection). If  $\alpha$  varies across the membrane, the algorithm is only slightly more complicated: The new coordinate and velocity  $(x^{n+1}, v^{n+1})$  are computed assuming that the friction varies in space, i.e., with the inertial convention for the average friction during the time step [Eq. (7)]. The step is accepted for  $R < P_{\text{cross}}$  and is changed to a reflection step for  $R > P_{\text{cross}}$ . In the latter case, one must take into account the fact that the particle has not passed the membrane and, therefore, the friction coefficient along its trajectory remains constant. Therefore, the new coordinate and velocity are recalculated using the G-JF algorithm, with the already chosen value of  $\beta^{n+1}$ , but with the friction coefficient at the initial coordinate  $x^n < x_m$ . The recalculated  $(x^{n+1}, v^{n+1})$  are accepted if the particle has not crossed the membrane ( $x^{n+1} < x_m$ ), and changed to  $(2x_m - x^{n+1}, -v^{n+1})$  if it has.

Fig. 2 shows simulation results for the PDF of a particle, initially located right next at a reflecting wall at

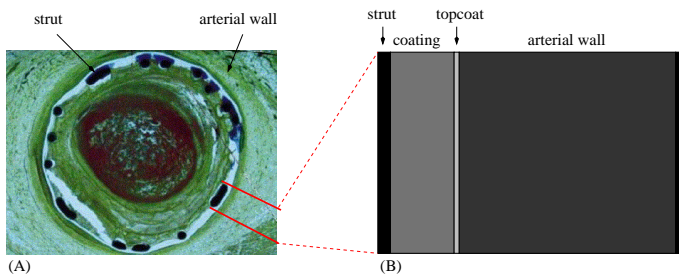


FIG. 3: (A) A cross section of a stented artery, and (B) the corresponding one-dimensional two-layer model for drug release from the stent to the artery.

$x = 0$ , and diffusing in a medium with constant  $D = 1$  that has a semi-permeable membrane at  $x_m = 10$ . The PDF at  $t = 100$  is plotted for various values of  $P_{\text{cross}}$ . The PDF is discontinuous at  $x_m$  because the membrane interferes with the diffusion rates. However, the membrane is not a probability sink or source and, therefore, the probability flux,  $j(x) = -D\partial_x P(x, t)$ , arriving at the membrane from left ( $x \rightarrow x_m^-$ ) is the same as the flux leaving the membrane to the right ( $x \rightarrow x_m^+$ ). This last feature of the PDF is visually apparent in Fig. 2. Since the membrane (partially) blocks the drug flow only from left to right, the probability density drops across the membrane, i.e.,  $P(x_m^-, t) > P(x_m^+, t)$ . The data in Fig. 2 suggests that the following relation holds:  $P_{\text{cross}} = P(x_m^+, t)/P(x_m^-, t)$ . This relation is anticipated from the continuity of the flux and the fact that for each  $P_{\text{cross}}$  molecules crossing the membrane from left to right, one molecule passes from right to left. For  $P_{\text{cross}} = 1$ , the membrane is effectively non-existent because it does not impede the diffusion. In this limit,  $P(x, t)$  becomes continuous at  $x_m$  and is given by Eq. (9) with  $x_0 = 0$  (solid line in Fig 2).

## IV. TWO-LAYER STENT MODEL

### A. The model

Fig. 3 (A) shows a cross section of a stented artery with the struts in contact with the arterial wall. Fig. 3(B) illustrates the mapping of the system to the simple one-dimensional model discussed herein. The model consists of two layers representing, respectively, the coating and the arterial wall. The first layer (coating), which has length  $L_1$ , is bounded between the stent strut ( $x = -L_1$ ) and the stent topcoat ( $x = 0$ ). The former is a reflecting boundary, while the latter is a thin semi-permeable membrane. The second layer (the arterial wall) is of length  $L_2$ . It is bounded between the topcoat and the adventitial side of the arterial wall ( $x = L_2$ ), which is modeled as an absorbing boundary since the drug arriving at the end of the artery is lost in the tissues adjacent to the adventitia. The first and second layers have diffusion co-

| parameter | physical value                        | normalized value      | simulation value |
|-----------|---------------------------------------|-----------------------|------------------|
| $L_1$     | $5 \times 10^{-6}$ m                  | 1                     | 1                |
| $L_2$     | $10^{-4}$ m                           | 20                    | 20               |
| $D_1$     | $10^{-17}$ m <sup>2</sup> /s          | 1/700                 | 1/700            |
| $D_2$     | $7 \times 10^{-15}$ m <sup>2</sup> /s | 1                     | 1                |
| $k_B T$   | $4.3 \times 10^{-21}$ J               | 1                     | 1                |
| $m$       | $1.5 \times 10^{-24}$ kg              | $6.8 \times 10^{-19}$ | 1                |
| $\tau_1$  | $2.5 \times 10^6$ s                   | 700                   | 700              |
| $\tau_2$  | $1.4 \times 10^6$ s                   | 400                   | 400              |
| $\tau_m$  | $3.5 \times 10^{-18}$ s               | $9.7 \times 10^{-22}$ | 1/700            |

TABLE I: Model parameters and their physical (second column), normalized (third column), and simulation (fourth column) values.

efficients  $D_1$  and  $D_2$ , respectively. We denote by  $m$  the mass of a drug molecule, and use the thermal energy  $k_B T$  as the energy scale of the problem.

Typical values for the system parameters are given in the second column of Table I in MKS units. In the third column, the same parameters are given in normalized units, where  $L_1 = 1$ ,  $D_2 = 1$ , and  $k_B T = 1$ . Table I also gives the physical and normalized values of the time scales  $\tau_i = L_i^2/D_i$  ( $i = 1, 2$ ), which are the characteristic diffusion times in each layer. Notice the interesting feature that these two time scales are of the same order of magnitude.

### B. Using a fictitious mass

Another characteristic time scale appearing in table I is  $\tau_m = mD/k_B T$ , which is the crossover time from inertial to diffusive Langevin dynamics. This time scale, to be henceforth referred to as the *ballistic time*, is very important from a computational perspective since Langevin dynamics simulations with the inertial interpretation must be run with time step  $dt < \tau_m$  in order to appropriately simulate the transition statistics between the layers. In multi-layers systems, the limit on  $dt$  is set by the most viscous layer with the smallest diffusion coefficient and the smallest ballistic time. Therefore, in table I, we only give  $\tau_m$  of the first layer. For the stent model, we have  $\tau_m \sim 10^{-18}$  sec, which is more than 24 orders of magnitude smaller than the diffusion times  $\tau_1$  and  $\tau_2$ . This poses a huge computational challenge, as the aim of the study is to measure quantities like the rate of drug transfer to the bloodstream, which require simulations on time scales comparable to  $\tau = \tau_1 + \tau_2$ . This implies that each simulated trajectory requires, at least,  $10^{24}$  time-steps, which would make the simulations prohibitively time consuming. More specifically, simulations of just  $10^4$  trajectories would require  $10^{13}$  years (!) of CPU time on a state of the art PC.

The key to circumvent this outstanding computational problem is to notice that the diffusion equation (1) and Langevin's equation (2) yield the same long-time probability distributions if Einstein's relation  $D(x)\alpha(x) = k_B T$  is satisfied. The mass of the particle, which only appears in Eq. (2), is unimportant for this relationship between the two equations to hold. Therefore, if we are only interested in obtaining the PDF at time scales comparable to  $\tau$ , we can use a fictitious mass which is much larger than the actual mass and, thus, artificially increase the ballistic time  $\tau_m$ . Of course, the artificial ballistic time must still be much smaller than the diffusion time, but  $\tau_m$  does not need to be *negligibly* smaller than  $\tau$ . In the fourth column of table I we give the normalized values of the model parameters used in our Langevin dynamics simulations of the DES model. The simulation values are identical to the normalized values for  $L_i$ ,  $D_i$ , and  $k_B T$ , but the mass in the simulations is set to unity, i.e., about 18 orders of magnitude larger than the actual normalized mass of a drug molecule. This narrows the gap between the ballistic time and diffusion times to 5-6 orders of magnitude, and makes computationally feasible simulations of hundreds of thousands of trajectories with integration time-step  $dt \ll \tau_m$ .

### C. Membrane permeability

In section III we defined  $P_{\text{cross}}$  to be the left-to-right crossing probability of the membrane in one time step. Since the time step of the simulations is typically several orders of magnitude smaller than the physical time scales of interest ( $dt \ll \tau$ ), the crossing probability  $P_{\text{cross}}$  will generally be very small, which would considerably slow down the simulations. To circumvent this problem, as well as the problem arising from the difficulty to accurately estimate the crossing probability, we replace  $P_{\text{cross}}$  with a different measure for the membrane permeability - the permeation time  $T$ . The latter can be related to  $P_{\text{cross}}$  by noticing that each time the particle attempts to cross the membrane, it has probability  $P_{\text{cross}}$  to cross it and probability  $1 - P_{\text{cross}}$  to be reflected. Thus, the probability of passing the membrane at the  $k$ -th attempt is  $P_{\text{cross}}(1 - P_{\text{cross}})^{k-1}$ , and the corresponding crossing time (measured from the time of the first crossing attempt) is  $T_k = (k - 1)\Delta$ , where  $\Delta$  is the return time between successive crossing attempts. This argument demonstrates that the permeation times are geometrically distributed, with an average crossing time  $\langle T_k \rangle = \Delta(1 - P_{\text{cross}})/P_{\text{cross}}$ . In reality,  $\Delta$  is obviously not fixed but, itself, follows a certain continuous distribution. Therefore, the actual permeation time does not follow a discrete geometric distribution, but its continuous exponential analogue

$$p(t) = \frac{1}{T} \exp(-t/T), \quad (11)$$

where  $T$  is the characteristic permeation time. Similarly to its discrete counterpart  $\langle T_k \rangle$ ,  $T = \Delta(1 - P_{\text{cross}})/P_{\text{cross}}$ ,

but here  $\Delta$  denotes the *average* time between successive attempts. To account for the delay effect of a semi-membrane in simulations, we follow the trajectory of the particle assuming that the membrane is fully-permeable (i.e., as if there is no membrane present). At each crossing of the membrane we draw a random waiting time from the exponential distribution (11), and this delay time is simply added to cumulative time of the dynamics.

## V. RESULTS

The quantity of most interest for therapeutic applications is the rate of drug transfer from the stent coating to the arterial tissue. This can be characterized by the fractions  $\Pi_1(t)$  and  $\Pi_2(t)$  of drug present in the coating (layer 1) and the arterial wall (layer 2), respectively. These quantities are related to the PDF via

$$\Pi_1(t) = \int_{-L_1}^0 P(x, t) dx, \quad (12)$$

$$\Pi_2(t) = \int_0^{L_2} P(x, t) dx. \quad (13)$$

In simulations, each trajectory is terminated upon arrival to the arterial wall boundary, which implies that  $\Pi_1(t) + \Pi_2(t)$  is a monotonic function decreasing from unity at  $t = 0$  to zero at  $t \rightarrow \infty$ .  $\Pi_1(t)$  and  $\Pi_2(t)$  are simply identified with the fraction of trajectories that at time  $t$  arrive at some point within the coating and arterial wall layers, respectively.

Fig. 4 shows our computational results for  $\Pi_1$  (dashed curves) and  $\Pi_2(t)$  (solid curves) as a function of the time  $t$ . The results are based on  $2.1 \times 10^5$  trajectories simulated with time step  $dt = 10^{-4}$  which meets the requirement  $dt \ll \tau_m$  where  $\tau_m = 1/700$  is the ballistic time (see table I). The initial coordinates of these trajectories are chosen from a uniform distribution between  $x = 0$  and  $x = L_1$ , which reflects the initial uniform distribution of the drug within the coating layer. The thin curves in Fig. 4 depict results for the DES model without a semi-permeable membrane, i.e., with vanishing permeation time  $T = 0$  between the layers. Not surprisingly,  $\Pi_1$  decreases monotonically from 1 to 0 on a time scale  $t \sim 10^3$  (roughly a month and a half in physical units), which is comparable to the sum of diffusion times in the coating and the arterial wall  $\tau = \tau_1 + \tau_2$ .  $\Pi_2$  increases from an initial value of 0, arrives to a maximum value for  $t \lesssim 200$ , and then monotonically decreases to 0 at larger times. The behavior of  $\Pi_2$  reflects net drug transfer from the stent coating to the arterial wall at the beginning of the process, followed by gradual loss of drug at longer times, due to absorption in the tissues adjacent to the adventitia. The thick curves in Fig. 4 depict results for the same model but with a semi-permeable membrane characterized by permeation time  $T = 10$ . The results for  $\Pi_1$  and  $\Pi_2$  in this case exhibit trends similar to those observed in the  $T = 0$  simulations. Importantly, we again

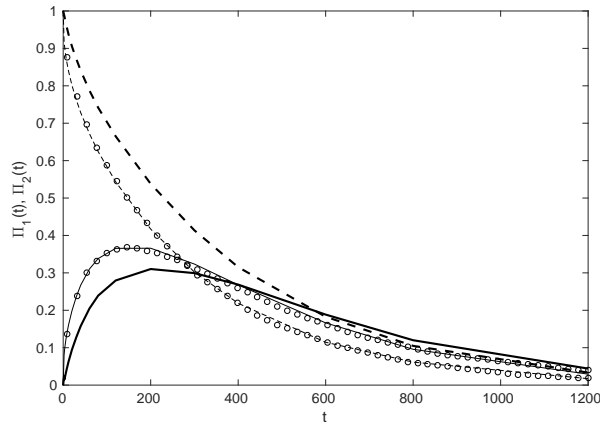


FIG. 4: The fraction of drug in the coating (dashed curves),  $\Pi_1$ , and in the arterial wall (solid curves),  $\Pi_2$ , as a function of time. The thin and thick curves show simulation results for a DES with semi-permeable membranes having, respectively, characteristic permeation times  $T = 0$  (no membrane) and  $T = 10$ . The circles represent the results of ref. [6] for the same DES model with identical model parameters (see footnote [45])

observe a decrease in the amount of drug left in the stent as a function of time and a non-monotonic behavior of the amount of drug found in the artery.

The open circles in Fig. 4 depict the results derived in ref. [6] for the same DES model with identical model parameters (see footnote [45]). These results have been obtained by numerically solving the diffusion equation at each layer, subject to a similar initial condition at  $t = 0$ , and boundary conditions at  $x = -L_1$  and  $x = L_2$ . At  $x = 0$ , the author of ref. [6] imposed (i) continuity of the flux and (ii) discontinuity in the concentration, with the concentration jump related, via the Kedem-Katchalsky (KK) equation [29], to the local flux and the membrane permeability. Explicitly, in ref. [6] [Eq. (2.11) therein] the KK equation is written in the following dimensionless form

$$\frac{\partial c_2}{\partial x} = \phi \left( c_2 - \frac{c_1}{\sigma} \right), \quad (14)$$

where  $c_1$  and  $c_2$  are the local concentrations on the left and right sides of the membrane, while  $\phi$  and  $\sigma$  are two transport coefficients depending on properties of the two media and the permeability of the interface. This continuum equation can be related to the particle-based Langevin simulations in the following manner: Consider a small time interval small  $dt$ , during which a particle residing on the left (stent) side of the membrane has a probability  $Q_1$  to cross the membrane, while a particle located on the right (artery) side has a crossing probability  $Q_2$ . The crossing probabilities are proportional to the diffusivities of the corresponding media, and  $Q_1$  also depends on the permeability of the membrane. The flux across the membrane is given by the

difference  $J = v_0[Q_1P(0-, t) - Q_2P(0+, t)]$ , where  $v_0$  is a proportionality coefficient with dimensionality of velocity. Since the flux is also given by  $J = -D_1\partial_x P(0-, t) = -D_2\partial_x P(0+, t)$ , we can also write

$$\frac{\partial P(0+, t)}{\partial x} = \frac{Q_2 v_0}{D_2} \left[ P(0+, t) - \frac{Q_1}{Q_2} P(0-, t) \right] \quad (15)$$

which has the same form as the KK equation for the boundary condition (14).

The results of ref. [6] exhibit a perfect agreement with our Langevin dynamics simulation results for  $T = 0$ . The agreement highlights the fact (which was not sufficiently discussed in previous studies of the model) that the DES membrane has a nearly negligible effect on the rate of drug flow from the stent coating to the arterial wall. The rate of drug release from the stent can be computed by numerical differentiation of  $\Pi_1(t)$  (12) with respect to time. The perfect agreement of our simulation results for  $\Pi_1(t)$  with ref. [6] indicates that the rate of drug release decreases monotonically with time (see Fig. 6 therein).

## VI. DISCUSSION

In this work we use underdamped Langevin dynamics simulations for solving the diffusion equation for a simple two-layer model of a drug-eluting stent (DES). To the best of our knowledge, this is the first attempt to derive the solution of a DES model using this approach. In fact, the application of underdamped Langevin dynamics simulations is also highly uncommon in other engineering and natural science areas dealing with the solution of complex diffusion equations. Much more common is the use of finite element and finite difference methods. These exist in a variety of forms, and the selection, design, and implementation of a method that best fits a given problem may be a complicated task. Langevin dynamics simulations constitute an alternative approach; however, the vast majority of studies of diffusion problems are based on simulations of the overdamped Langevin equation which neglect the inertial term on the r.h.s. of Eq.(2). This introduces complications stemming from the Itô-Stratonovich dilemma and the associated spurious drift. These complications can be addressed when  $D(x)$  is a smooth function which varies only slightly during an integration time step, but not in simulations of layered systems where  $D(x)$  is discontinuous. In the latter case, one must introduce decision rules for crossing the boundary between layers, even if those layers are *not* separated by a membrane. A Monte-Carlo algorithm implementing such types of decision rules has been recently presented [46], but we are not aware of a similar algorithm for overdamped Brownian dynamics. This extraordinary problem is completely avoided in underdamped Langevin dynamics simulations which, if run properly, produce correct thermal diffusion between sharp interfaces. Accurate solutions for a wide range of diffusion equations can be obtained by this approach with relative

computational simplicity and accuracy, provided that one uses a robust integration scheme (such as the G-JF integrator) together with a suitable convention rule for choosing the average  $\alpha$  within a time-step of the simulations (e.g., the “inertial” convention). The merits of the approach are nicely exemplified in Fig. 4, which exhibits perfect agreement between the simulation results of this paper and the predictions of ref. [6] for the same model.

The only parameter that needs to be tuned in the simulations is the mass of the diffusing particle whose value does not affect the PDF at the large time scales of interest associated with the diffusion problem. It must be selected such that the ballistic time  $\tau_m = m/\alpha$  is much smaller, but not necessarily negligible, compared to the characteristic diffusion time. In one-dimensional multi-layer systems, the ballistic time is set by the friction coefficient of the most viscous layer, and the inertial convention for the average friction needs to be applied only when the particle moves between layers. However, the method can be readily implemented to diffusion problems in higher dimensions and can, without any special difficulty, be employed to study systems where the diffusion coefficient changes continuously in space. Such problems are generally more complicated for analytical treatment, as well as for other computational approaches.

The model studied in this paper encompasses only two aspects of pharmacokinetics in the DES system, namely diffusion and crossing of a semi-permeable membrane. More recent studies suggest that advection, caused by a pressure gradient and blood circulation, and drug binding to receptor sites within the arterial wall may have a substantial effect on the rate of drug transport [14]. Both mechanisms can be dealt with within the underdamped Langevin dynamics simulation method presented in this work. Specifically, advection results from the action of a deterministic (“regular”) force acting on the particle in addition to friction and thermal noise. In the presence

force, the full form of G-JF discrete-time equations must be used (see equations (21)-(22) in [35])

$$x^{n+1} = x^n + bdtv^n + \frac{bdt}{2m}\beta^{n+1} + \frac{bdt^2}{2m}f^n, \quad (16)$$

$$v^{n+1} = av^n + \frac{b}{m}\beta^{n+1} + \frac{dt}{2m}(af^n + f^{n+1}), \quad (17)$$

which include appropriate additional terms missing in equations (3) and (4). Drug binding can be dealt with by distributing binding sites and introducing a short-range attractive potential between the diffusing particle and the binding sites. The forces associated with the gradient of the binding potentials can then be accounted for via Eqs. (16) and (17). In a future publication we plan to investigate model systems including these additional effects, in order to demonstrate the great potential of underdamped Langevin dynamics simulations for solving non-trivial diffusion problems.

We conclude by restating that although this work deals with the problem of drug diffusion from a DES, the larger goal of the paper is to advocate underdamped Langevin dynamics simulations as an efficient and simple to implement method for solving diffusion problems in heterogeneous environments. The method is based on computation of an ensemble of single particle stochastic trajectories with small time steps that are in the inertial regime. This does not render the method useless for studying problems where the time scales of interest are well in the diffusive regime. Quite the contrary, if one is only interested in diffusive behavior, the mass of the simulated particles can be assigned a fictitious value (see details in section IV B) to allow for faster simulations with larger time steps.

We thank MD Carlos Cafri for helpful discussions about physiological aspects of the problem.

- 
- [1] Safian R.D., Textor S.C. (2001) Renal-Artery Stenosis. *N Engl J Med*, 344, 431-442.
  - [2] Dotter C.T., Buschman R.W., McKinney M.K. (1983) Transluminal expandable nitinol stent grafting: Preliminary report. *Radiology*, 147, 259-260.
  - [3] Costa M.A., Abizaid A., Sousa A.G.M.R., Sousa J.E. (2007) Chapter 22 in *Essentials of Restenosis For the Interventional Cardiologist*. Duckers H.J., Nabel E.G. and Serruys P.W., editors. Totowa NJ: Human Press.
  - [4] Joner M., Finn A.V., Farb A., Mont E.K., Kolodgie F.D., Ladich E., et al. (2006) Pathology of drug-eluting stents in humans: delayed healing and late thrombotic risk. *J Am Coll Cardiol*, 48, 193-202.
  - [5] Roguin A. (2011) Stent: The Man and Word Behind the Coronary Metal Prosthesis. *Circulation: Cardiovascular Interventions*, 4,206-209.
  - [6] Pontrelli G., de Monte F. (2007) Mass diffusion through two-layer porous media: an application to the drug-eluting stent. *Int J Heat Mass Transf*, 50, 3658-3669.
  - [7] Vergara C., Zunino P. (2008) Multiscale boundary conditions for drug release from cardiovascular stents. *M.M.S*, 7, 565-588.
  - [8] Pontrelli G., de Monte F. (2010) A multi-layer porous wall model for coronary drug-eluting stents. *Int J Heat Mass Transf*, 53, 3629-3637.
  - [9] McGinty S. (2014) A decade of modeling drug release from arterial stents. *Math Biosci*, 257, 80-90.
  - [10] Pontrelli G., de Monte F. (2014) A two-phase two-layer model for transdermal drug delivery and percutaneous absorption. *Math. Biosci*, 257, 96-103.
  - [11] McGinty S., Vo T.T.N., Meere M., McKee S., McCormick C. (2015) Some design considerations for polymer-free drug-eluting stents: A mathematical approach. *Acta Biomaterialia*, 18, 213-225.
  - [12] McGinty S., Pontrelli G. (2015) A general model of coupled drug release and tissue absorption for drug delivery devices. *J. Control Release*, 217, 327-336.
  - [13] McGinty S, Wheel M, McKee S, McCormick C. (2015)

- Does anisotropy promote spatial uniformity of stent-delivered drug distribution in arterial tissue?. *Int J Heat Mass Transf*, 90, 266-279.
- [14] McGinty S., Pontrelli G. (2016) On the role of specific drug binding in modeling arterial eluting stents, Arterial paclitaxel distribution and deposition. *J Math Chem*, 54, 967-976.
- [15] Ferriera J.A., Naghipoor J., de Oliviera P. (2016) A coupled non-Fickian model of a cardiovascular drug delivery system. *Math Med Biol*, 33, 329-357.
- [16] Pontrelli G., de Monte F. (2009) Modeling of mass dynamics in arterial drug-eluting stents. *J Porous Media*, 12,19-28.
- [17] McGinty S., McKee S., Wadsworth R.M., McCormick C. (2011) Modeling drug-eluting stents. *Math Med Biol*, 28, 1-29.
- [18] D'Angelo C., Zunino P. (2011) Robust numerical approximation of coupled stokes' and darcy's flows applied to vascular hemodynamics and biochemical transport. *Esaim-Math Model Num*, 54, 447-476.
- [19] Hossain S.S., Hossain S.F.A., Bazilevs Y., Calo V.M., Hughes T.J.R. (2012) Mathematical modeling of coupled drug and drug-encapsulated nanoparticle transport in patient-specific coronary artery walls. *Comput Mech*, 45, 213-242.
- [20] Pontrelli G., Mascio A.D., de Monte F. (2013) Local mass non-equilibrium dynamics in multi-layered porous media: Application to the drug-eluting stent. *Int J Heat Mass Transf*, 66, 844-854.
- [21] Mandal A.P., Sarifuddin, Mandal P.K. (2015) An unsteady analysis of arterial drug transport from half-embedded drug-eluting stent. *Appl Math Comput*, 266, 968-981.
- [22] Seidlitz A., Nagel S., Semmling B., Grabow N., Martin H., Senz V. (2011) Examination of drug release and distribution from drug-eluting stents with a vessel-simulating flow-through cell. *Eur J Pharm Biopharm*, 78, 36-48.
- [23] McGinty S, McKee S, Wadsworth RM, McCormick C. (2013) Modeling arterial wall drug concentrations following the insertion of a drug-eluting stent. *Siam J Appl Math*, 73, 2004-2008.
- [24] Hickson R.I., Barry S.I., Mercer G.N. (2009) Critical times in multilayer diffusion. Part 1: Exact solutions. *Int J Heat Mass Transf*, 52, 5776-5783.
- [25] Hickson R.I., Barry S.I., Mercer G.N. Critical (2009) times in multilayer diffusion. Part 2: Approximate solutions. *Int J Heat Mass Transf*, 52, 5784-5791.
- [26] d'Errico M., Sammarco P., Vairo G. (2015) Analytical modeling of drug dynamics induced by eluting stents in the coronary multi-layered curved domain. *Math Biosci*, 267, 79-96.
- [27] Rodrigo M.R., Worthy A.L. (2016) Solution of multilayer diffusion problems via the Laplace transform. *J Math Anal Appl*, 444, 475-502.
- [28] Grassi M., Pontrelli G., Teresi L., Grassi G., Comel L., Ferluga A., et al. (2009) Novel design of drug delivery in stented arteries: A numerical comparative study. *Math Biosci*, 6, 493-508.
- [29] Zunino P. (2004) Multidimensional pharmacokinetic models applied to the design of drug-eluting stents. *Cardiov Eng: Int J*, 4, 181-191.
- [30] Garon A., Delfour M.C. (2014) Three-dimensional quadratic model of paclitaxel release from biodegradable polymer films. *Siam J Appl Math*, 74, 1354-1374.
- [31] Creel C., Lovich M., Edelman E. (2000) Arterial paclitaxel distribution and deposition. *Circ Res*, 86, 879-884.
- [32] Hwang C., Wu D., Edelman E.R. (2011) Physiological transport forces govern drug distribution for stent-based delivery. *Circulation*, 104, 600-605.
- [33] O'Connell B.M., Walsh M.T. (2010) Demonstrating the Influence of Compression on Artery Wall Mass Transport. *Ann Biomed Eng*, 38, 1354-1366.
- [34] Lovich M., Edelman E. (1995) Mechanisms of transmural heparin transport in the rat abdominal aorta after local vascular delivery. *Circ Res*, 77, 1143-1150.
- [35] Grønbech-Jensen N., Farago O. (2013) A simple and effective Verlet-type algorithm for simulating Langevin dynamics. *Mol Phys*, 111, 983-991.
- [36] Langevin P. (1908) On the theory of Brownian motion. *C R Acad Sci (Paris)*, 146:530-533.
- [37] Einstein A. (1905) Investigation on the theory of Brownian movement. *Ann Phys (Leipzig)*. 17, 549-560.
- [38] Farago O., Grønbech-Jensen N. (2014) Fluctuation-dissipation relation for systems with spatially varying friction. *J Stat Phys*, 156, 1093-1110.
- [39] Farago O., Grønbech-Jensen N. (2014) Langevin dynamics in inhomogeneous media: Re-examining the Itô-Stratonovich dilemma, *Phys Rev E*, 89, 013301.
- [40] Regev S., Grønbech-Jensen N., Farago O. (2016) Isothermal Langevin dynamics in systems with power-law spatially dependent friction. *Phys Rev E*, 94, 012116.
- [41] Grønbech-Jensen N., Hayre N.R., Farago O. (2014) Application of the G-JF discrete-time thermostat for fast and accurate molecular simulations. *Comput Phys Commun*, 185, 524-527.
- [42] Itô K. (1944) Stochastic integral. *Proc Imp Acad*, 20, 519-524 .
- [43] Stratonovich R.L. (1966) A new representation for stochastic integrals and equations. *Siam J Control*, 5, 362-371.
- [44] Coffey W.T., Kalmykov Y.P., Waldron J.T. (1966) *The Langevin Equation With Applications to Stochastic Problems in Physics, Chemistry and Electrical Engineering*, Hackensack NJ: World Scientific Publishing Company.
- [45] The only model parameters not having identical values to those in [6] are the layers diffusion coefficients  $D_1$  and  $D_2$  whose values here are  $10^3$  times smaller than in [6]. The values quoted in [6] correspond to characteristic diffusion times  $\tau_1$  and  $\tau_2$  that are unrealistically low (hours rather than weeks). The values of  $D_1$  and  $D_2$  used here agree with more recent estimates, see e.g. [9]. This change does not affect the comparison of our solution for  $\Pi_1(t)$  and  $\Pi_2(t)$  with the data visually extracted from Fig. 3 in ref. [6], because the results throughout this paper are plotted in normalized units. Notice that the definition of the normalized time unit is different here ( $\tau_2 = 400$ ) than in ref. [6] ( $\tau_2 = 1$ ). The data from [6] is plotted in Fig. 4 after conversion to the time units used in this work (i.e., multiplication by a factor of 400).
- [46] H.W. de Haan. M.V. Chubynsky. (2012) Monte Carlo Approaches for Simulating a Particle at a Diffusivity Interface and the "Itô-Stratonovich Dilemma. *cond-mat preprint*: arXiv:1208.5081..